ISBN: 978-3-95450-240-0 ISSN: 2673-5539 doi:10.18429/JACoW-RuPAC2021-MOY01

THE NICA COMPLEX INJECTION FACILITY

A. Butenko †, H. Khodzhibagiyan, S. Kostromin, I. Meshkov, A. Sidorin, E. Syresin, G. Trubnikov, A. Tuzikov, Joint Institute for Nuclear Research, Dubna, Russia

Abstract

The Nuclotron-based Ion Collider fAcility (NICA) is under construction in JINR. The NICA goals are providing of colliding beams for studies of hot and dense strongly interacting baryonic matter and spin physics. The NICA complex injection facility consists of following accelerators: Alvarez-type linac LU-20 of light ions up to 5 MeV/u; heavy ion linac HILAC with RFQ and IH DTL sections at energy 3.2 MeV/u; superconducting Booster synchrotron at energy up 578 MeV/u; superconducting synchrotron Nuclotron at gold ion energy 3.85 GeV/u. In the nearest future the old LU-20 will be substituted by a new light ion linac for acceleration of 2<A/z<3 ions up to 7 MeV/u with additional two acceleration sections for protons, first IH section for 13 MeV and the second one - superconducting for 20 MeV. The status of NICA injection facility is under discussion.

NICA INJECTION COMPLEX

The NICA accelerator complex [1,2] is constructed and commissioned at JINR. NICA experiments shall be performed in search of the mixed phase of baryonic matter and nature of nucleon/particle spin. The new NICA accelerator complex will permit implementing experiments in the following modes: with the Nuclotron ion beams extracted at a fixed target; with colliding ion beams in the collider; with colliding ion-proton beams; with colliding beams of polarized protons and deuterons. The main elements of the NICA complex are an injection complex, which includes a set of ion sources and two linear accelerators, the superconducting acting Booster, the superconducting acting synchrotron Nuclotron, a Collider composed of two superconducting rings with two beam interaction points, a Multi-Purpose Detector (MPD) and a Spin Physics Detector (SPD) and beam transport channels.

The injection complex [1] is divided on two injection chains: one is used for heavy ions, other - for protons and light ions. The light ion injection chain includes laser ion source (LIS) and source of polarized ions (SPI), linear accelerator LU-20, Nuclotron and transfer line LU-20-Nuclotron. The heavy ion injection chain consists from electron string ion source (ESIS), laser ion source, plasma ion source, the acting Heavy Ion Linac (HILAC), transfer line HILAC-Booster, superconducting acting synchrotron Booster, transfer line Booster-Nuclotron and acting superconducting synchrotron Nuclotron.

INJECTION CHAIN FOR LIGHT IONS

The linear accelerator LU-20, which is under operation since 1974, accelerates protons and ions from few sources: the laser source and the source of polarized ions - protons and deuterons. SPI was constructed by JINR-INR RAS collaboration. The beam current of polarized deuterons corresponds to 2 mA. During 2009 - 2018 years completely modernized all of the main systems of the Linac: RF power amplifiers (5MW/pulse), drift tubes power supply (PS), beam diagnostics, HV terminal, fore-injector, LLRF system, synchronization system, vacuum system, PS system of the injection line. At the LU-20 exit, the energy of ions is 5 MeV/n. At present time, the LU-20 beam is injected directly into the Nuclotron through transfer line Lu-20-Nuclotron. The HV injector of linac LU-20 has been replaced in 2016 by RFQ (Fig. 1) [1,3] with beam matching channels. The RFQ was constructed by JINR, ITEP of NRC "Kurchatov Institute", NRNU MEPHI, VNIITF collaboration. The new buncher constructed by ITEP of NRC "Kurchatov Institute" was installed between RFQ and LU-20 in 2017. Installation of new buncher permited to increase the heavy ion beam current by 5 times in Nuclotron 55 run in 2018.

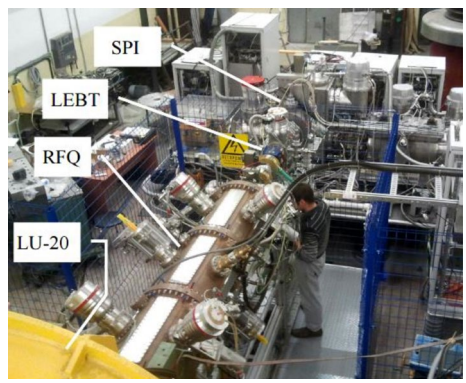

Figure 1: New fore-injector for LU-20.

The design of new Light Ion Linac (LILAc) was started in 2017 to replace the LU-20 in NICA injection complex. LILAc consists of three sections: warm injection section applied for acceleration of light ions and protons up to energy 7 MeV/n [4], warm medium energy section used for proton acceleration up to energy 13 MeV [4] and superconducting HWR sections [5], which provides proton acceleration up to energy 20 MeV. The LILAC should provide beam current of 5 emA. The construction of first light ion section [4] at ion energy 7 MeV/n was started in 2018 by Bevatech (Germany), it should be delivered in JINR in 2023. The next step of the LILAc project – design of a middle energy section and HWR superconducting sections.

The increased beam energy of LILAc is required for future researches with polarized proton beams. The operating frequency of the LILAc is equal to 162.5 MHz for first two sections and 325 MHz for HWR section. The two superconducting HWRs (Fig. 2) were constructed by Russian-Belarusian collaboration with participation of JINR, NRNU MEPhI, INP BSU and PTI NASB.

ISBN: 978-3-95450-240-0 ISSN: 2673-5539 doi:10.18429/JACoW-RuPAC2021-MOY01

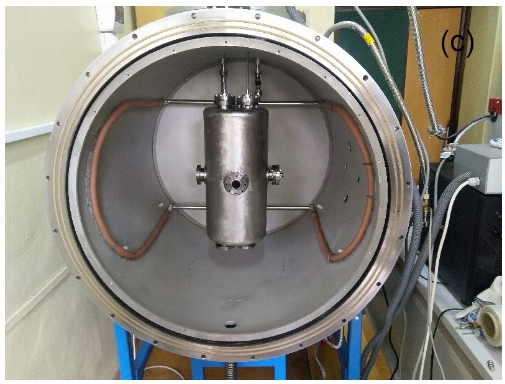

Figure 2: Niobium cavity inside of testing cryostat.

INJECTION CHAIN FOR HEAVY IONS

The second linear accelerator of NICA injection complex— a new heavy-ion linear accelerator (Heavy Ion Linac, HILAc) [1,6] (Fig. 3) constructed by JINR-Bevatech collaboration is under exploitation since 2016. It is aimed to accelerate heavy ions injected from KRION-6T, a superconducting electron-string heavy ion source. At the present time KRION-6T produces 5×10^8 Au^{31+} and 2×10^8 $^{209}Bi^{27+}$ ions.

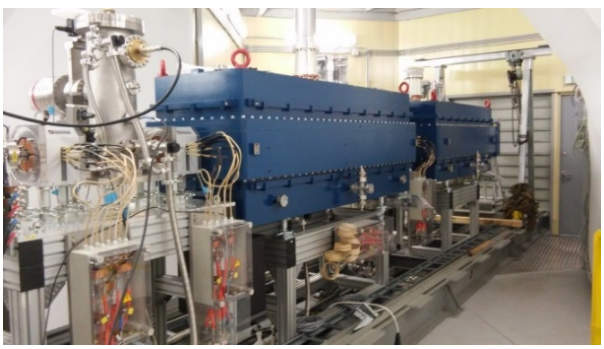

Figure 3: Heavy ion linear accelerator.

This ion source will be used at injection in Booster in 2022. Upgraded version of KRION-N with $^{197}Au^{31+}$ or $^{209}Bi^{35+}$ ion intensity up 2×10^9 particles per pulse will be constructed in 2022 for Collider experiments. The energy of ions at the exit from HILAc is 3.2 MeV/n, while the beam intensity amounts to 2×10^9 particles per pulse or 10 emA, repetition rate is 10 Hz. The HILAc consists of three sections: RFQ and two IH sections. The RFQ is a 4-rod structure operating at 100.625 MHz. The RFQ and each IH section are powered by 140 kW and 340 kW solid state amplifiers.

Especially for the test of the Booster [7] the plasma source generating a single component He^{1+} beam was created. The efficiency of beam transportation through second and third IH sections was 78.5% (Fig. 4). The maximal ion $^4He^{1+}$ beam current at HILAC entrance during first Booster runs corresponds to project value 10 mA. During second Booster run the $^4He^{1+}$and $^{56}Fe^{14+}$ ions produced in plasma and laser ion sources were accelerated in HILAC and injected in Booster.

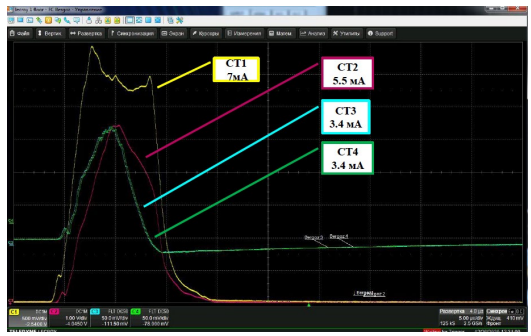

Figure 4: Signals of current transformers CT: CT1 at RFQ exit, CT2 at IH2 exit, CT2-at the middle of transfer line HILAC-Booster, CT3 at transfer line exit.

The transfer line from HILAC to Booster (Fig. 5) [8] consists of 2 dipole magnets, 7 quadrupole lenses, 6 stirrers magnets, debuncher, collimator, vacuum and diagnostic equipment. The debuncher constructed by Bevatech reduces relative ion momentum spread after HILAc from 5×10^{-3} to 10^{-3}. The collimation diaphragm in transport channel provides separation of ions with required charge $^{197}Au^{31+}$ from parasitic ions with another charges. The assembling of transfer line was done in 2020. The achieved efficiency of beam transportation during first Booster beam run was of 90% at beam current at the HILAC exit of 4 mA, this value was sufficient for the first experiments [7]. The measured beam profiles (Fig. 6) is in agreement with beam sizes obtained from channel optic simulations.

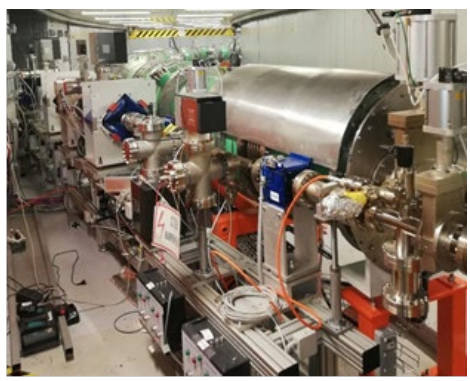

Figure 5: Transport channel HILAC-Booster.

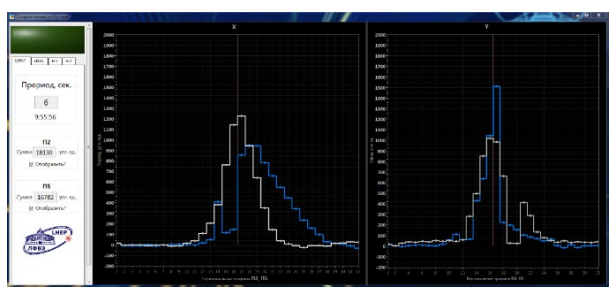

Figure 6: Beam profiles measured by PM2 and PM5.

The Booster [1] is a superconducting synchrotron intended for accelerating heavy ions to an energy of 600 MeV/n. The magnetic structure of the Booster with a 211-m-long circumference is mounted inside the yoke of the Synchrophasotron magnet.

ISBN: 978-3-95450-240-0 ISSN: 2673-5539 doi:10.18429/JACoW-RuPAC2021-MOY01

Figure 7: Booster ring inside Synchrophasatron yoke.

The main goals of the Booster are accumulation of $2 \cdot 10^9$ Au^{31+} ions, acceleration of heavy ions up to the energy 578 MeV/n required for effective stripping, and forming of the required beam emittance with the electron cooling system. The Booster has a four-fold symmetry lattice with DFO periodic cells. Each quadrant of the Booster has ten dipole magnets, six focusing and six defocusing quadrupole lenses, and multipole corrector magnets. All Booster dipole magnets and quadrupole lenses were fabricated and tested at JINR.

The Booster power supply system provides consecutive connection of dipole magnets, quadrupole focusing and defocusing lenses. The main powerful source of the power supply system forms a current of up to 12.1 kA with the required magnetic field ramp of 1,2 T/s. Two additional power supply sources are intended for flexible adjustment of the Booster working point.

The beam injection system of the Booster consists of an electrostatic septum and three electric kickers.

The Booster RF system provide 10 kV of acceleration voltage. The operating frequency range of the stations is from 587 kHz to 2526 kHz.

The electron cooling system has the maximal electron energy of 60 keV.

The Booster beam extraction system consists of a magnetic kicker, two magnetic septa, a stripping station and a closed orbit bump subsystem. The ions accelerated in the Booster are extracted and transported along a magnetic channel, and on their way, they cross a stripped target. The channel consists of five dipole magnets, eight quadrupole lenses, three correctors, separation septa, and diagnostic and vacuum equipment.

The installation of the Booster cryomagnetic equipment (Fig. 7) was started in September 2018. The first technical Booster run was done in November-December 2020.

At the first stage the insulating vacuum volume and beam pipe were assembled and tested. After this the cooling of cryomagnetic system, commissioning of thermometry, quench protection systems, tuning of power supply and HILAC-Booster beam transfer line systems were done. Then the beam was injected into the Booster [7] on the plateau of the magnetic field corresponding to the injection energy. The beam circulation was achieved without activation of the orbit correction system.

Turn-by-turn measurements were used for the injection optimization. The signals from two nearest BPMs and virtual model of the injection section permitted to calculate linear optics and closed orbit position in the injection point depending on the quadrupole settings (Fig. 8). The efficiency of beam pass through injection section was achieved at the level of about 75%.

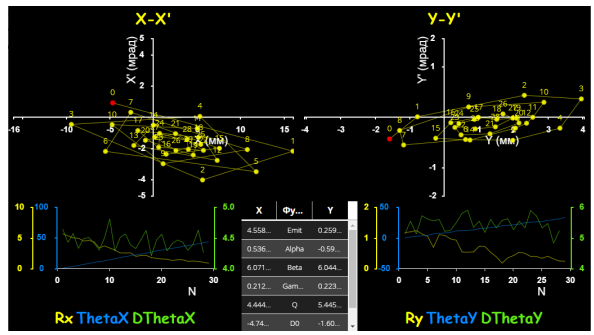

Figure 8: Turn-by-turn measurements of the linear optics and closed orbit position in the injection point.

After the orbit correction and tuning of the injection system the intensity of the $^4He^{1+}$ circulating beam was increased up to 7×10^{10} ions (Fig. 9). The charge of these ions is equal to charge of 2×10^9 Au^{31+} ions. Life time of ions corresponds to 1.3 s or equivalent average residual gas pressure 2×10^{-8} Pa.

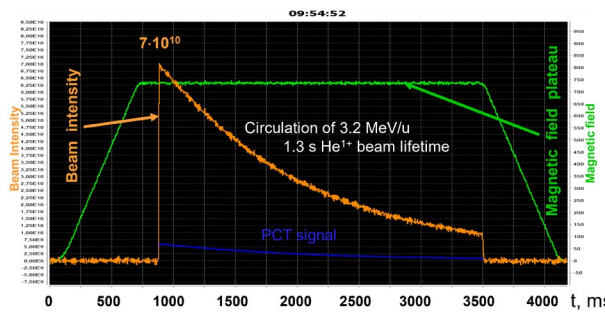

Figure 9: PCT signal, beam intensity and magnetic field time dependencies during the cycle.

The beam current transformer signal at ion acceleration up energy of 100 MeV/n is shown in Fig. 10. The choice of maximal ion energy was defined by the radiation safety conditions at Booster operation without beam extraction.

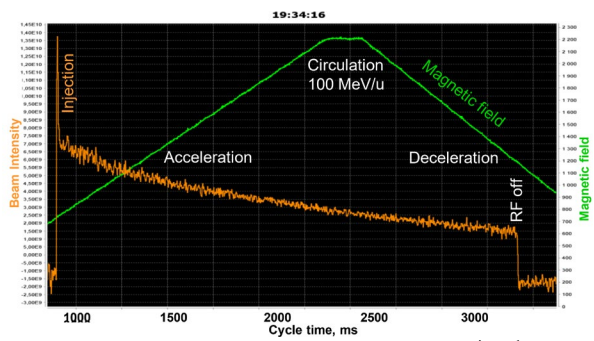

Figure 10: Beam current transformer signal at $^4He^{1+}$ ion acceleration.

During second run of the Booster in September 2021 the beams of ions $^4He^{1+}$ and $^{56}Fe^{14+}$ with mass-to-charge ratio A/Z=4 and intensity up 4×10^{10} and 4×10^8 correspondently were injected in to the Booster, bunched on the injection

ISBN: 978-3-95450-240-0 ISSN: 2673-5539 doi:10.18429/JACoW-RuPAC2021-MOY01

table of magnetic field on fifth RF harmonic, then accelerated up to 65 MeV/u where recaptured with first RF harmonic and again accelerated. The $^{56}Fe^{14+}$ ions were accelerated up to project energy – 578 MeV/n (Fig. 11).

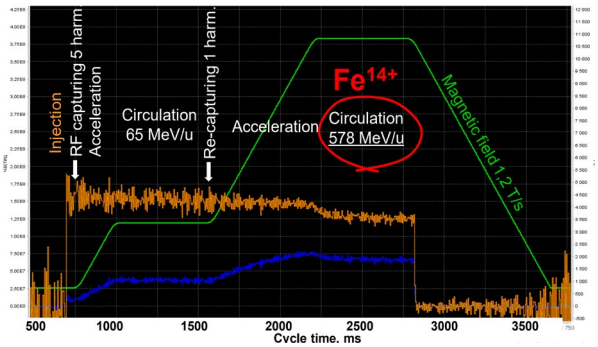

Figure 11: Beam current transformer signal at $^{56}Fe^{14+}$ ion acceleration.

The main results of the second cycle of the Booster beam commissioning are following: the beam injection efficiency with adiabatic capturing at 5 harmonic at efficiency is higher than 95%; accelerating up to 65 MeV/u, where recaptured with 1 RF harmonic with efficiency closed to 100%; acceleration up to project energy of 578 MeV/u with dB/dt = 1.2 T/s; ultra-high vacuum in beam pipe ($^{4}He^{+1}$ ion life-time more than 10 s), electron cooling of ions at energy 3.2 MeV/n, beam extraction to transfer line Booster-Nuclotron and transportation in this transfer line with total transfer efficiency of 70%.

The $^{4}He^{1+}$ ion life (Fig. 12) during second Booster run corresponds to 10.8 s. The equivalent residual gas pressure is about 5×10^{-9} Pa. The relative concentration of residual gases like CO and H_2O in warm Booster sections was several times less during second run in comparison with first one.

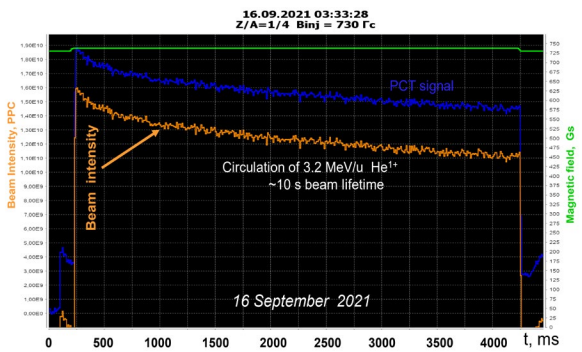

Figure 12: Beam current transformer signal at $^{4}He^{1+}$ ion energy 3.2 MeV/u.

The electron cooling of $^{56}Fe^{14+}$ ions was first time realized during second Booster run. The relative momentum spread of cooled ions is equal to 4×10^{-4}. Transverse cooling time at beam emittance reduction in e-times corresponds to 1,4 s.

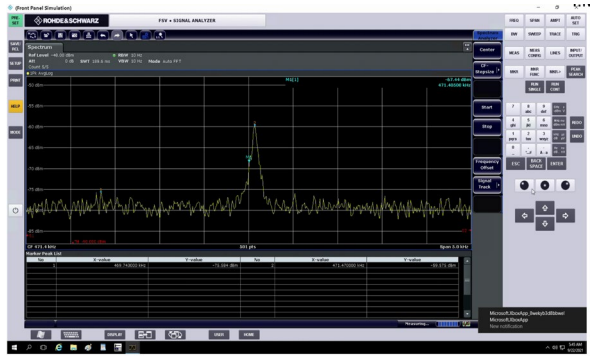

Figure 13: Schottky noise signal at 4 harmonic of revolution frequency and ion energy 3.2 MeV/u.

The cryomagnetic and power supply systems were tested at the design magnetic field cycle during first Booster run (Fig. 14). The magnetic cycle has three plateaus: for injection, electron cooling and beam extraction. The achieved ramping rate 1.2 T/s of the magnetic field corresponds to the project value (Fig. 14). The achieved maximum magnetic field of 1.8 T also equal to the project value.

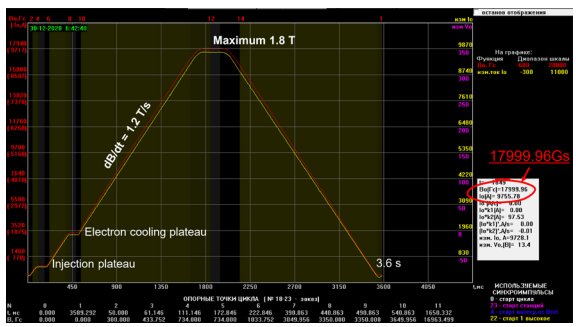

Figure 14: The Booster magnetic field cycle at design parameters.

The Booster beam extraction system [8] consists of a magnetic kicker, two magnetic septa, a stripping station and a closed orbit bump subsystem including four lattice dipoles with five additional HTS current leads. The Booster beam extraction system together with transfer line Booster-Nuclotron (Fig. 15) was fabricated by BINP SB RAS. The first beam experiments with extracted $^{4}He^{1+}$ and $^{56}Fe^{14+}$ ion beams were performed during second Booster beam run. The total efficiency of beam extraction from Booster and transportation in transfer line Booster–Nuclotron corresponds to about 70%.

Figure 15: The Booster-Nuclotron transfer line.

ISBN: 978-3-95450-240-0 ISSN: 2673-5539 doi:10.18429/JACoW-RuPAC2021-MOY01

THE NUCLOTRON

The linear accelerator LU-20, which is under operation

The upgraded Nuclotron [9] accelerates protons, polarized deuterons and ions to a maximum energy depending of the sort of particles. The maximum ion energy corresponds to 5.2 GeV/n at present time (Table 1).

Table 1: Main Parameters of Nuclotron Beams

Parameter	Project	Status, 2020
Max. magn. field, T	2	2 (1.7 routine)
B-field ramp, T/s	1	0.8 (0.7 routine)
particles	p – U, d↑	p↑, d↑, p – Xe
Maximum energy, GeV/u	12 (p), 5.8 (d) 4.5 $^{197}Au^{79+}$	5.2 (d, C), 3.6 (Ar^{16+})
Intensity, ions/cycl	10^{11} (p,d), 2×10^{9} (A > 100)	d 4×10^{10} (2×10^{10} routine) $^{7}Li^{3+}3\times10^{9}$ C^{6+} 2×10^{9} $Ar^{16+}1\times10^{6}$ $Kr^{26+}2\times10^{5}$ $Xe^{42+}1\times10^{4}$

The polarized deuteron beams were obtained at intensity up 2×10^{9} ppp in Nuclotron runs 53 and 54 with SPI in 2016-2018 (Table 1). The polarized proton beams were formed first time at intensity 10^{8} ppp in Nuclotron 54 run in 2017. The injection with RF adiabatic capture at efficiency of 80%. was used in two last Nuclotron runs 54 and 55 in 2017 and 2018. The run 55 in 2018 was performed with acceleration of C^{6+}, Ar^{16+} and Kr^{26+} (Fig.16) ion beams (Table 1). The resonant stochastic extraction (RF knockout technique) was realized in the run 55 in 2018.

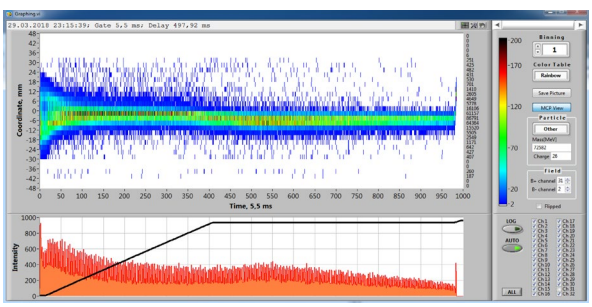

Figure 16: The size and beam intensity of extracted from Nuclotron Kr^{26+} ion beam.

The installation in the Nuclotron of the Booster beam injection system and the Collider fast extraction system are required for its operation as the main synchrotron of the NICA complex. The kicker and Lambertson magnet (Fig. 17) should be installed for injection section in end 2021 or in beginning 2022.

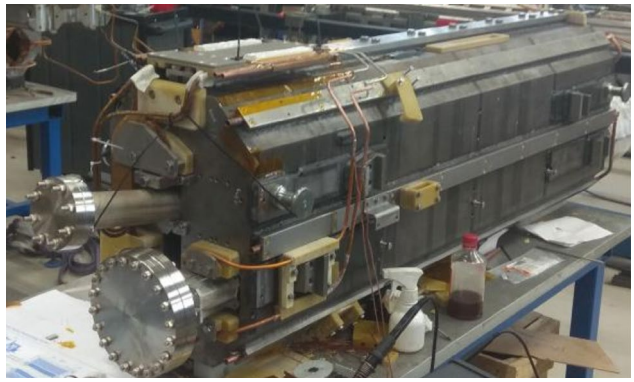

Figure 17: The Nuclotron Lambertson magnet for injection section.

REFERENCES

[1] Technical Project of NICA Acceleration Complex, Dubna, 2015.

[2] V.D. Kekelidze R. Lednicky, V.A. Matveev *et al.*, Three stages of the NICA accelerator complex, *Eur. Phys. J. A*, v.52:211, p.390, 2016. doi:10.1088/1742-6596/668/1/012023

[3] V.A. Andreev, A.I. Balabin, A.V. Butenko *et al.*, *Problems of Atomic Science and Technology. Series: Nuclear Physics Investigation*, v.6, no7, pp.943-946, 2016.

[4] H. Höltermann, M. Basten, B. Koubek *et al.*, "Light Ion Linear Accelerator up to 7 AMeV for NICA", in *Proc. RuPAC'18*, Protvino, Russia, Oct. 2018, paper WECAMH02, pp. 68-71. doi: 10.18429/JACoW-RUPAC2018-WECAMH02.

[5] D. Bychanok, A Sukhotski, S Huseu *et al.*, "Control of electromagnetic properties during prototyping, fabrication and operation of low-β 325 MHz half-wave resonators", *Journal of Physics D: Applied Physics*, vol. 54, no. 10, p. 255502, Apr. 2021. doi:10.1088/1361-6463/abf168.

[6] A.M. Bazanov, A.V. Butenko, B.V. Golovenckiy *et al.*, "Commissioning of the new heavy ion linac at the NICA project, in *Proc.IPAC17*, Copenhagen, Denmark, May 2017, paper TUPVA116, pp.2362-2364.

[7] A. Butenko, N. Agapov, A. Alfeev *et al.,* "First Experiments with Accelerated Ion Beams in the Booster of NICA Accelerator Complex", presented at the *12th Int. Particle Accelerator Conf. (IPAC'21),* Campinas, Brazil, May 2021, paper MOPAB025.

[8] A.V. Butenko, V.I. Volkov, C. Yu. Kolesnikov *et al.,* "Beam transport channels and beam injection and extraction systems of the NICA accelerator complex", *Nuclei and Letters*, v.13, pp.966-977, 2016. doi:10.1134/S1547477116070190.

[9] E.M. Syresin, N.N. Agapov, A.V. Alfeev *et al.*, "Nuclotron Development for NICA Acceleration Complex", in *Proc. IPAC 19*, Melbourne, Australia, May 2019, paper THXXPLM1, pp.3396-3398. doi: 10.18429/JACoW-IPAC2019-THXXPLM1